

Atomization and Powder Processing of High Temperature Ferritic Stainless Steel

Iver E. Anderson¹, Joel R. Rieken², David J. Byrd¹, and M.J. Kramer¹

¹Division of Materials Sciences and Engineering, Ames Laboratory (USDOE), Ames, IA

²Materials Science and Engineering Department, Iowa State University, Ames, IA

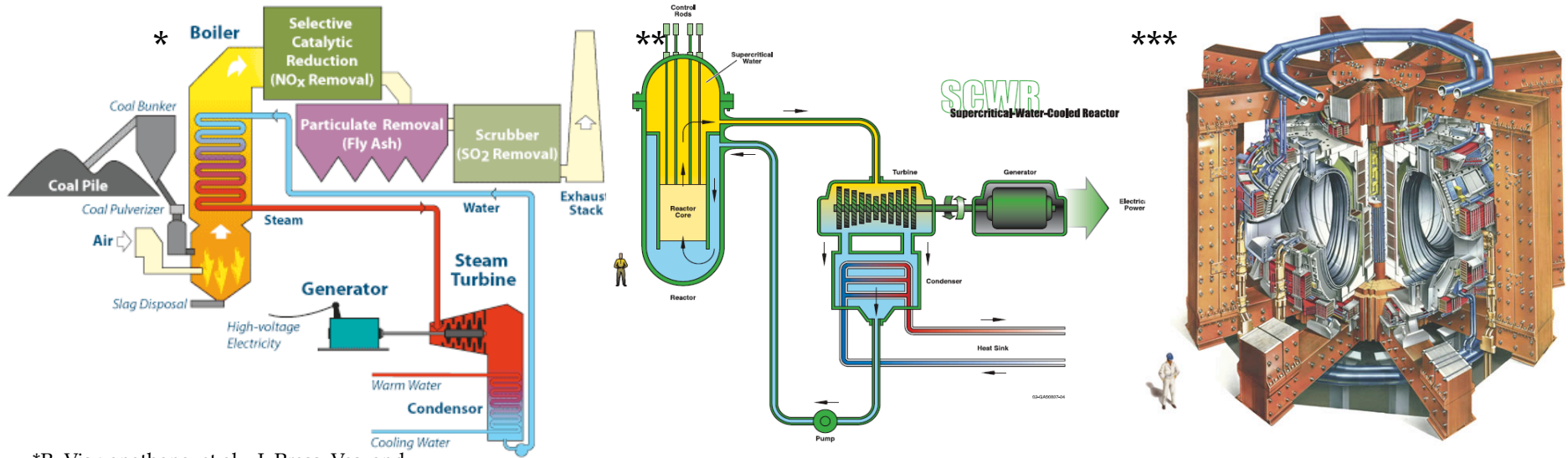
25th Annual Conference on Fossil Energy Materials

Portland, Oregon

April 26, 2011

Support from U.S. Department of Energy-Office of Fossil Energy is gratefully acknowledged through Ames Laboratory contract no. DE-AC02-07CH11358

Advanced Materials for Future Generation Power Plants



*R. Viswanathana, et al., J. Press. Ves. and Pip., 2006. 83: p. 778-783.

**U.S. DOE Nuclear Energy Research Advisory Committee, and Generation IV International Forum GIF, GIF-002-00 OECD Nuc. E. Agency, 2002: p. 1-90.

***ITER, *The ITER Device*. http://www.iter.org/a/index_nav_4.htm, 2009.

Material	Cost/kg (USD)	Notes
Ferritic Stainless Steel	~\$2-5	446 Plate form
Austenitic Stainless Steel	~\$3-7	316L Plate form
F/M Fe-9Cr steels	≤\$5.50	Plate form
Ni-based	~\$30-35	Inconel 718 Sheet (Special Metals), Inconel 617 (Special Metals)
Fe-based ODS	~\$165, ~\$345	MA956 Sheet (Special Metals), PM 2000 (Plansee)
V-4Cr-4Ti	~\$200	Plate form (Average between 1994 and 1996 US fusion program large heats)
SiC _f /SiC _m composites	~\$1000, ~\$200	Chemical vapor infiltration, and Chemical vapor reaction

ODS Processing Cost!

J.T. Busby, J. Nuc. Mat., 2009. 392: p. 304

K. Savolainen, J. Mononen, R. Ilola, and H. Hänninen, 2005, Helsinki University of Technology, Laboratory of Engineering Materials Publications.

S.J. Zinkle and N.M Ghoniem, Fusion Engineering and Design 2000. 51(52): p. 55-71. Special Metals Price Quote

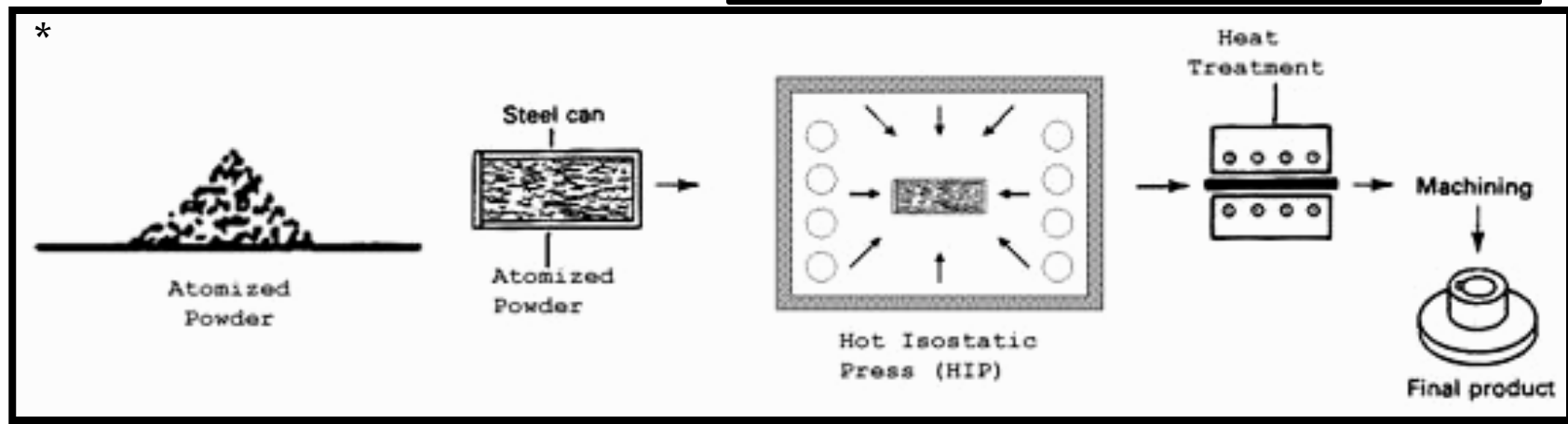
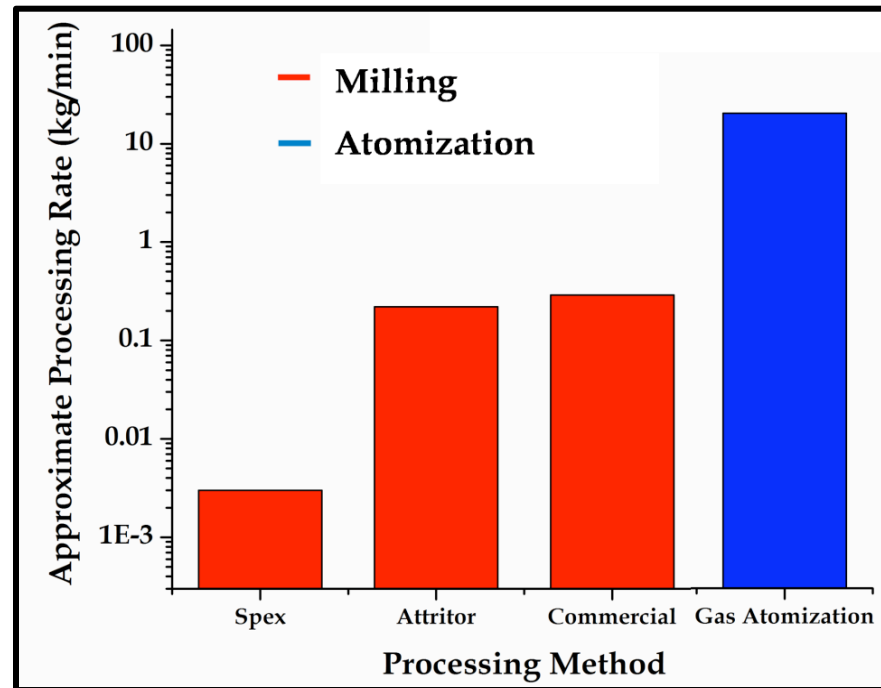
Fe-Based ODS Processing Comparison

* Mechanical Alloying

- Long milling times
- Batch commercial process (~2000 kg)
- Powder contamination (C, O, N, Ar)
- Anisotropic microstructure

** Gas Atomization (GARS + RSP)

- Higher processing rates (10-30 kg/min)
- Continuous processing capacity
- Minimized contamination
- Isotropic microstructure capability

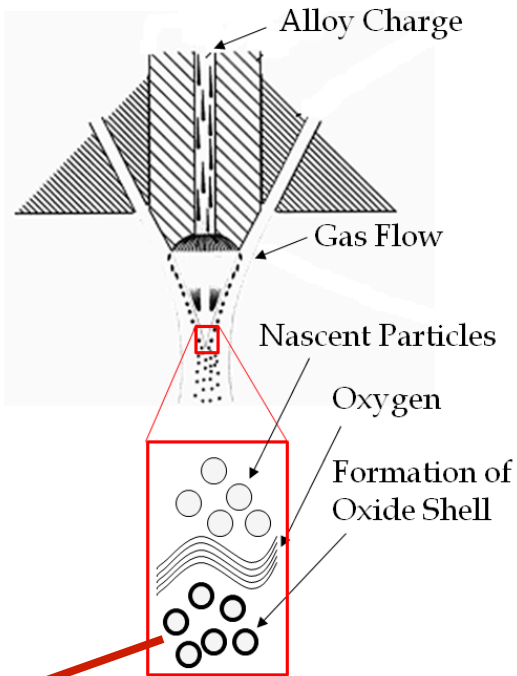
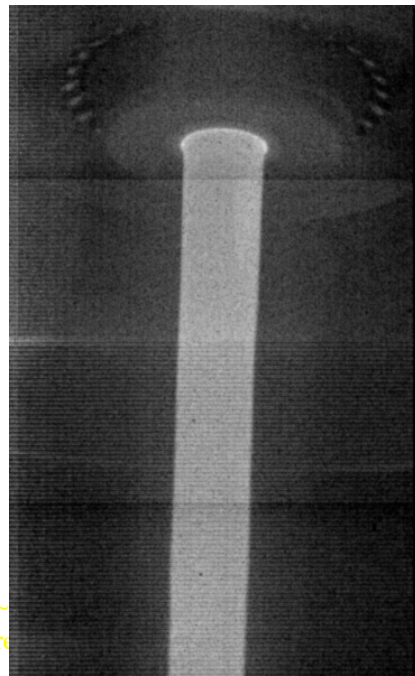


* R.L. Terpstra, et al., *Advances in Powder Metallurgy and Particulate Materials*, 2006.

*C. Suryanarayana, *ASM Handbook*, Vo. 7, ASM International, Materials Park, OH, 1998, pp. 80-90.

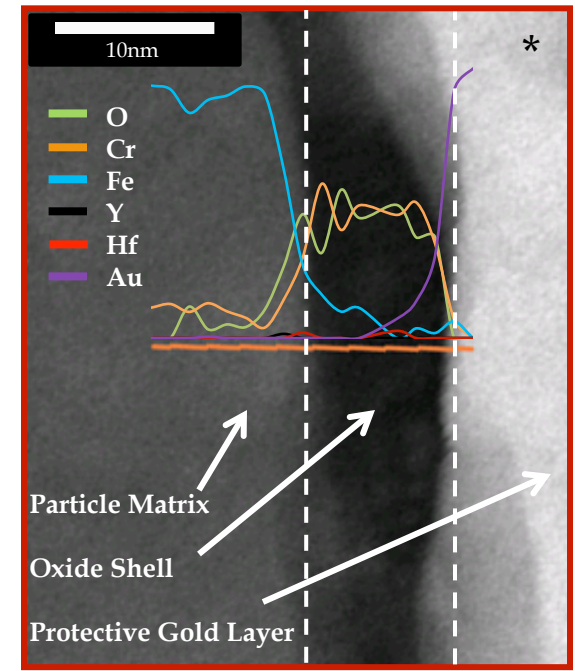
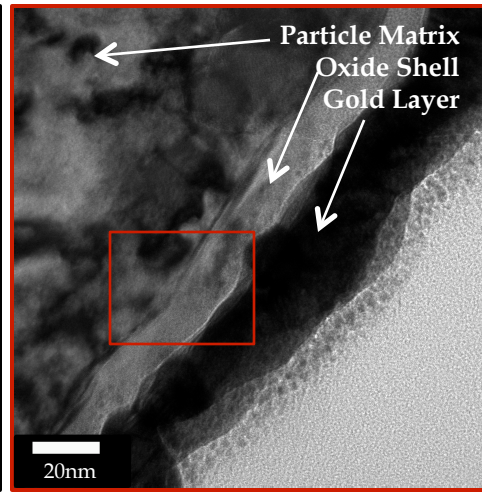
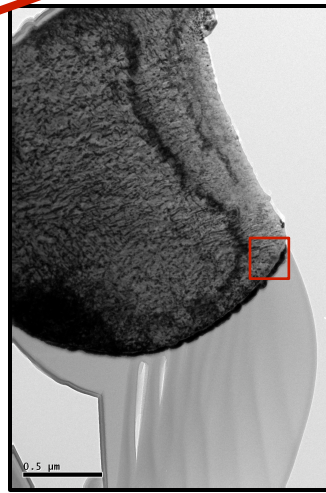
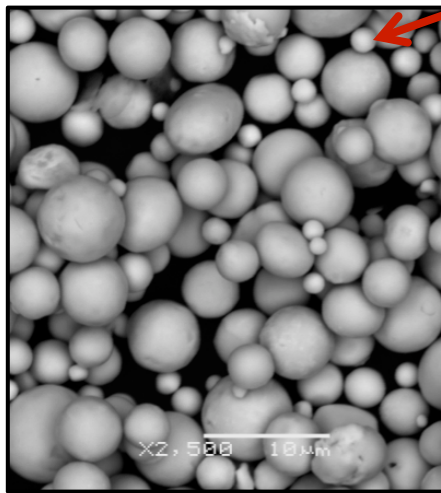
**R.M. German, *Powder Metallurgy and Particulate Materials Processing*, 2005, MPIF, Princeton, NJ

Gas Atomization Reaction Synthesis (GARS)



Fe-Cr-Y-Hf-O

Element	Basic Alloy Design	Approx. Conc. (at.%)
Cr	Surface reactant	15.0-16.0
Y	Nano-metric oxide dispersoid former	0.1-0.2
Hf	Dispersoid stabilizer	0.1-0.3
O ₂	Surface oxidant and dispersoid former	0.35-0.70

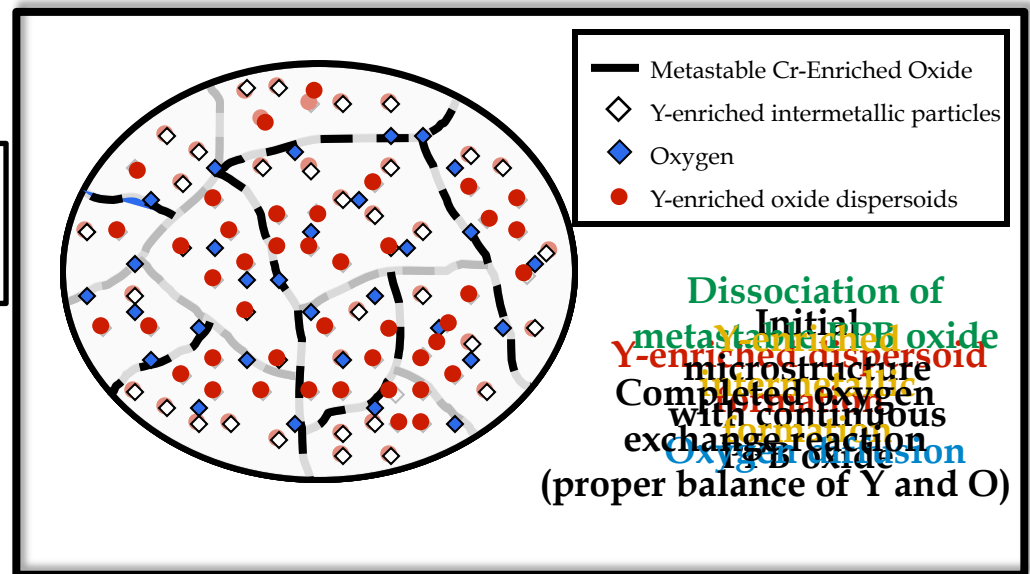
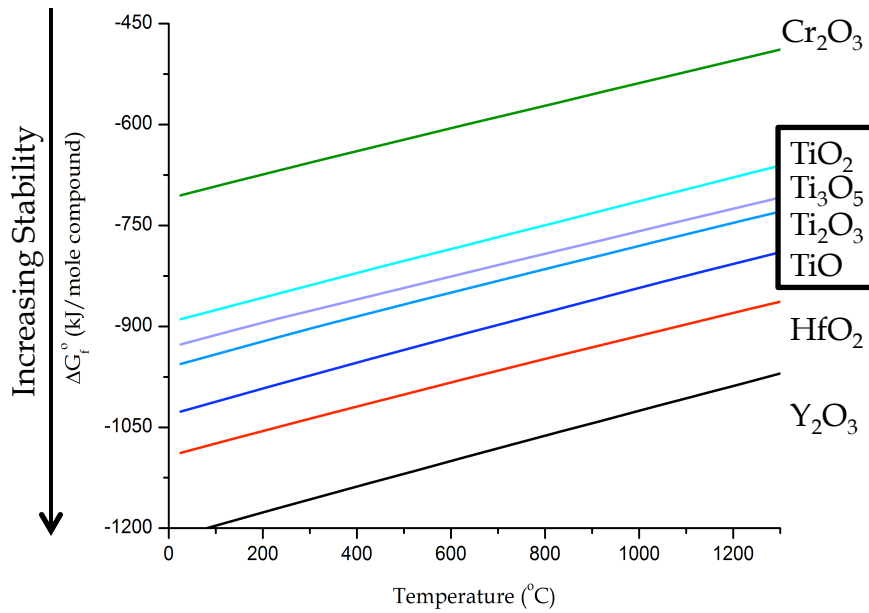
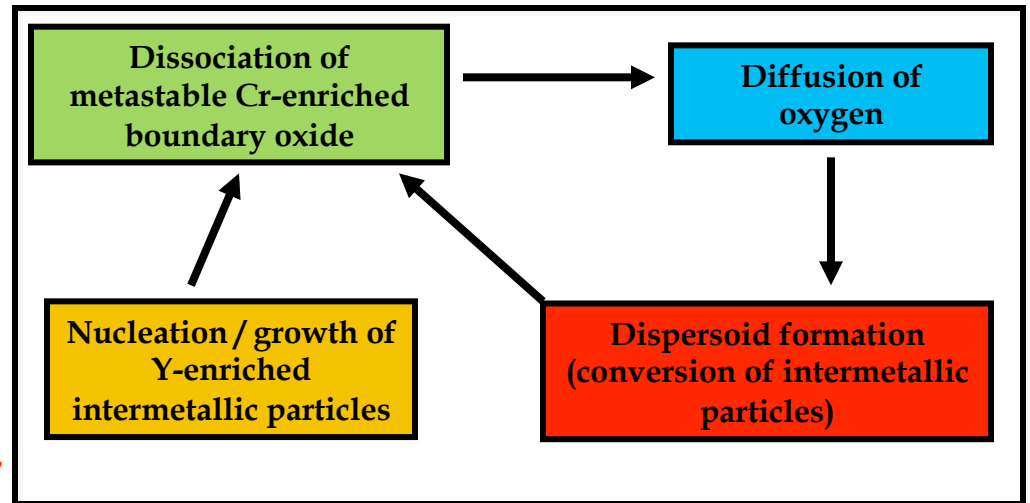


Dispersoid Formation Mechanism

Solid-State Microstructure Evolution

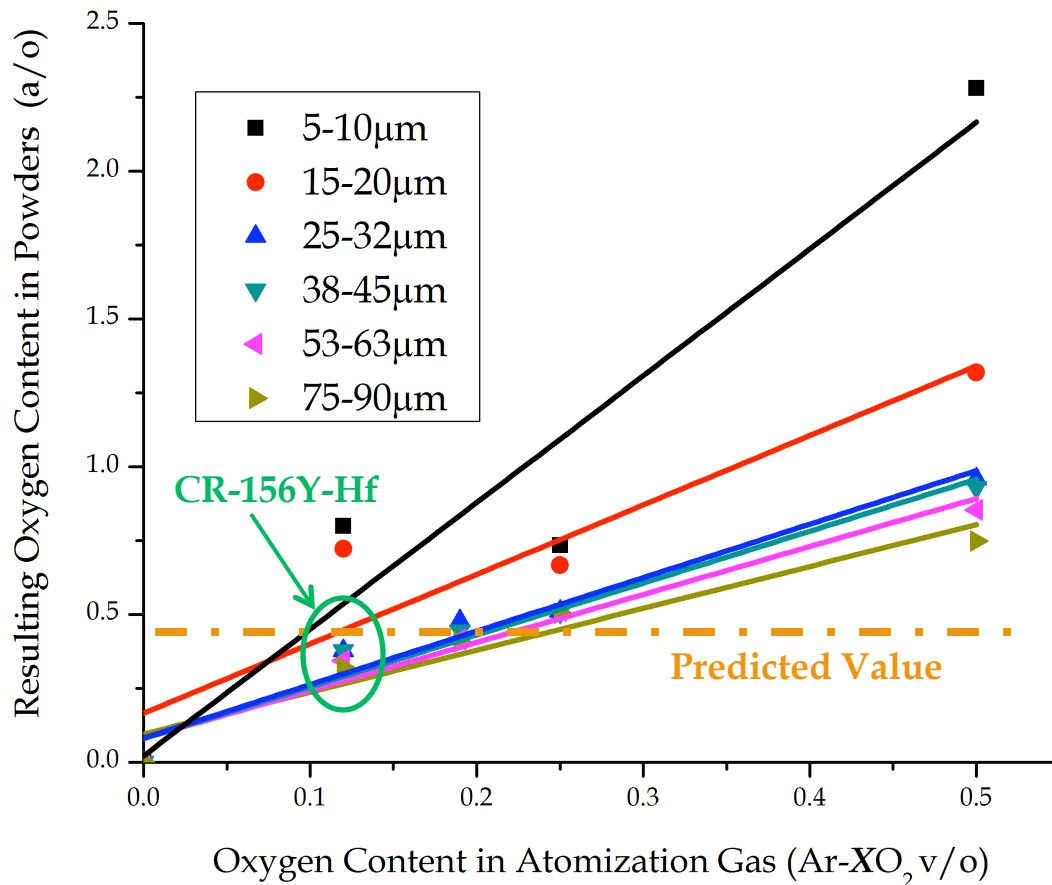
(Internal Oxygen Exchange Reaction)

- Nucleation / growth of Y-enriched intermetallic particles (solidification or low temperature HIP)
- Dissociation of metastable prior particle boundary Cr-enriched oxide
- Oxygen diffusion away from PPBs
- Nano-metric Y-enriched oxide formation
- *Full dissociation of PPB oxide will be necessary for ideal mechanical properties*

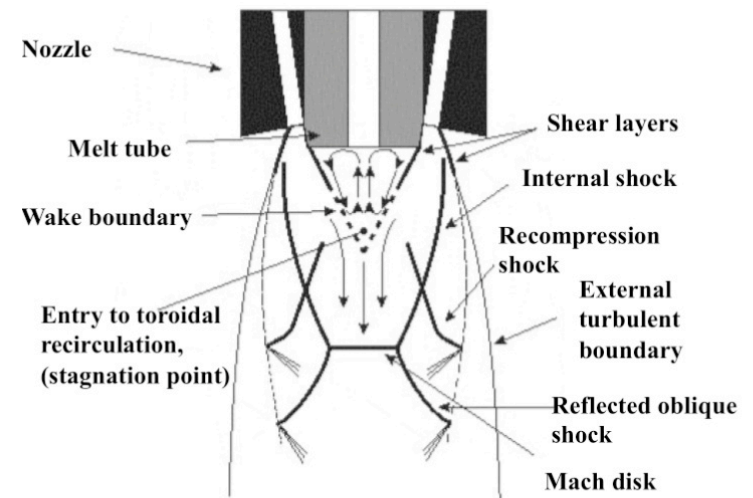


Reactive Atomization Process Control

Empirically developed GARS oxidation model



- **Rapid oxidation kinetics**
- **Primarily dependent on the mass flow rate of oxygen (local p_{O_2} within primary atomization zone)**
- **Sensitive to atomization parameters (i.e., gas nozzle and pour tube design)**

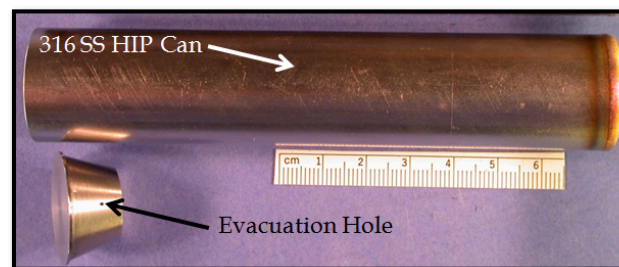
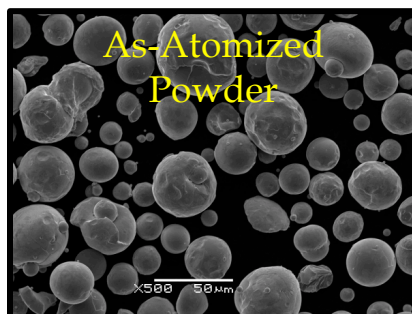
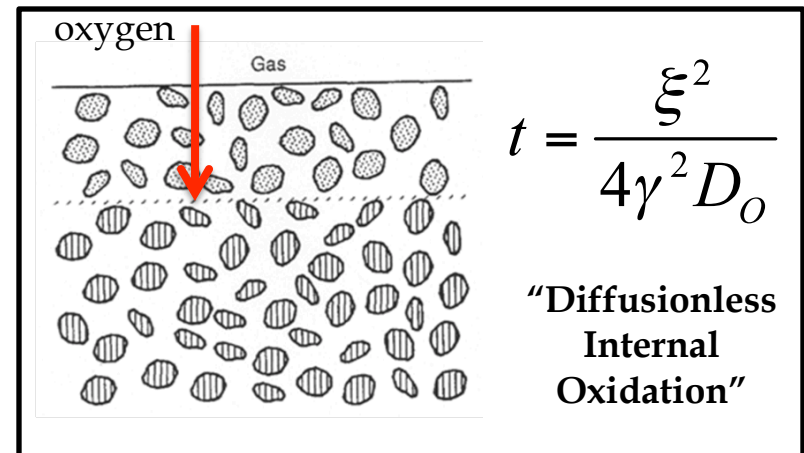


J. Ting and I.E. Anderson, Mat. Sci. Eng., A379 (2004), 264-276.

CR-Alloy Composition and Experimental Parameters

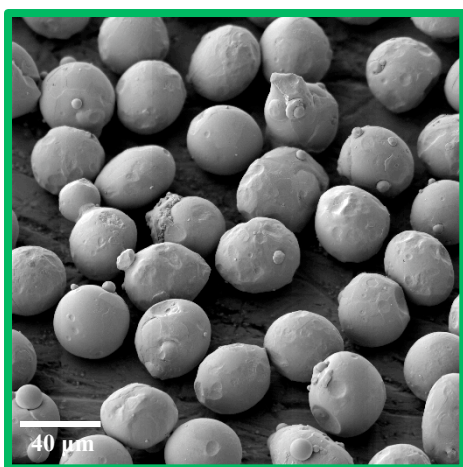
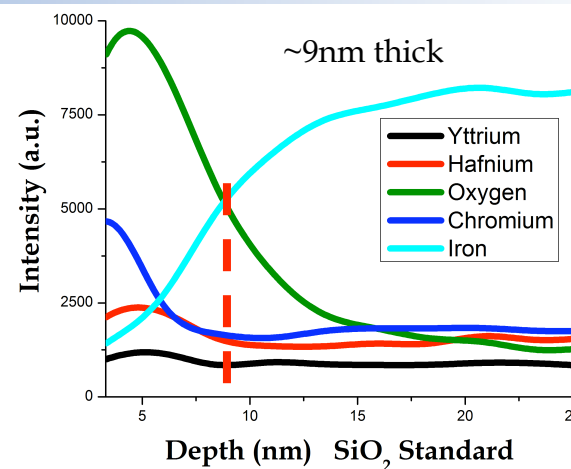
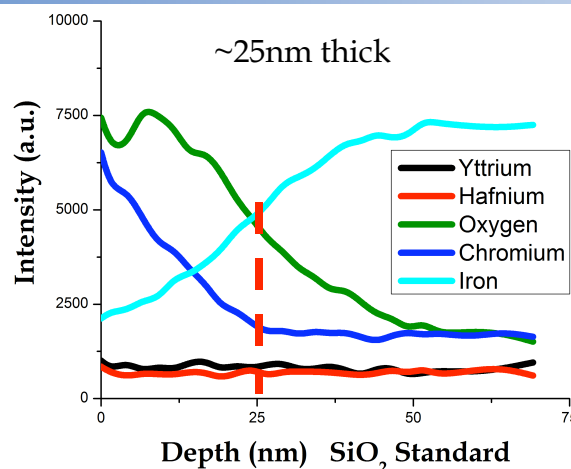
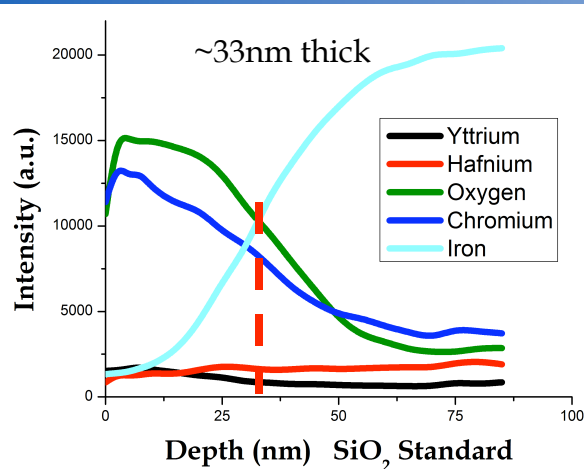
Alloy		Fe (at. %)	Cr (at. %)	Hf (at. %)	Y (at. %)	O (at. %)	Rxn Gas (vol.%)	Rxn Gas Inlet
CR-156YHf	Nominal	Bal.	16.0	<u>0.12</u>	<u>0.31</u>	-	Ar-0.12O ₂	HPGA Nozzle
CR-156YHf	20-53 μm	Bal.	15.84	<u>0.11</u>	<u>0.18</u>	<u>0.38</u>	Ar-0.12O ₂	HPGA Nozzle
CR-156YHf	5-20 μm	Bal.	15.84	<u>0.11</u>	<u>0.18</u>	<u>0.76</u>	Ar-0.12O ₂	HPGA Nozzle
CR-156YHf	-5 μm	Bal.	15.84	<u>0.11</u>	<u>0.18</u>	<u>1.45</u>	Ar-0.12O ₂	HPGA Nozzle

- Size classified Powders: <5, 5-20, 20-53 μm)
(Solidification microstructure)
- Low temperature consolidation (700°C-200MPa-4hr)
(Fe-Y intermetallic particle formation/distribution)
- Elevated temperature heat treatment (1200°C-2.5hr-Vac)
*Predicted from internal oxidation experiments
(Mixed nano-metric oxide dispersoid formation)

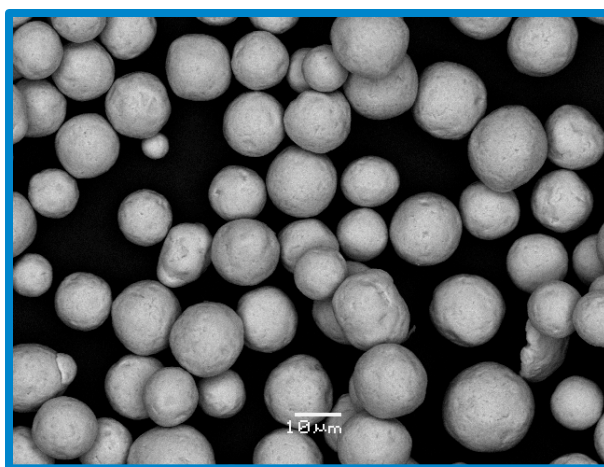


As-Atomized Surface Chemistry

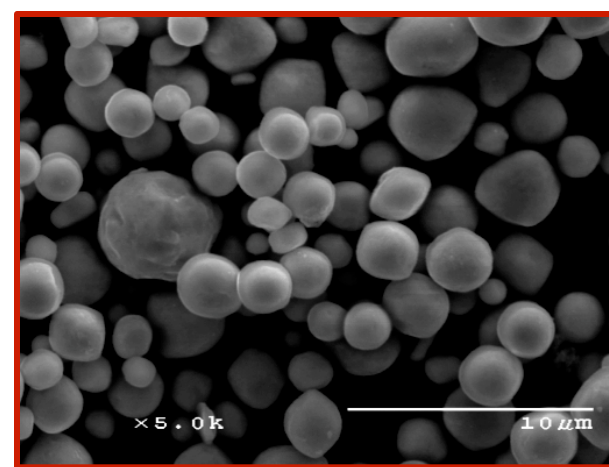
CR-156Y-Hf: Fe-15.84Cr-0.11Hf-0.18Y at.%



32-38 μm



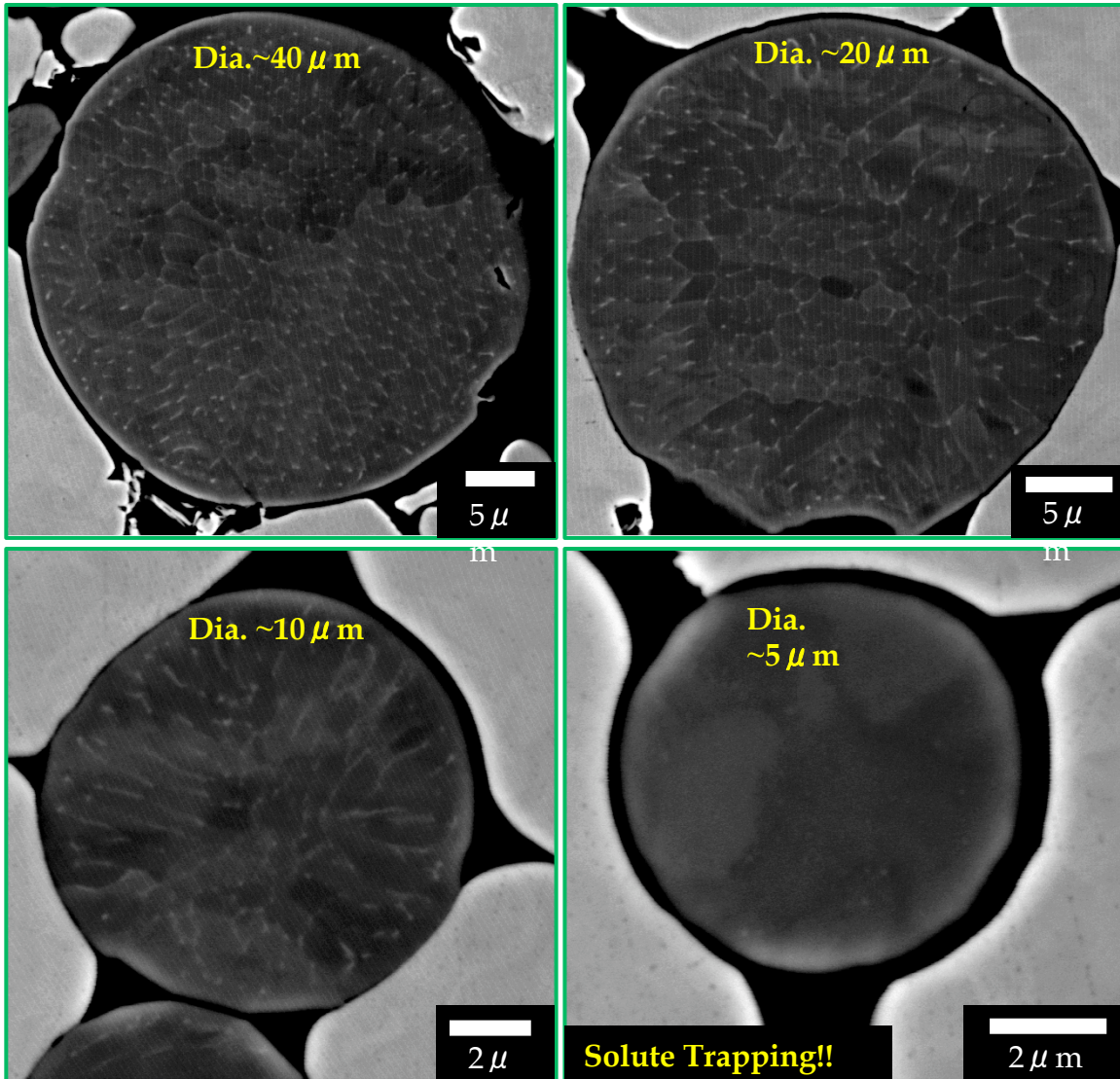
15-20 μm



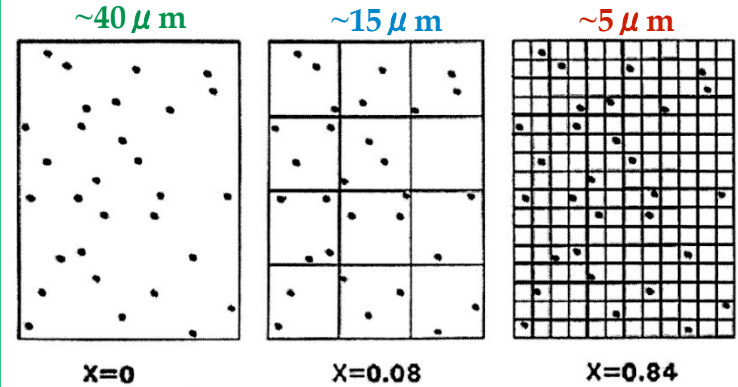
-5 μm

- Auger depth profiles show enrichment of O and Cr at powder surface
- Oxide shell thickness decreases with powder size (cooling rate sensitive)

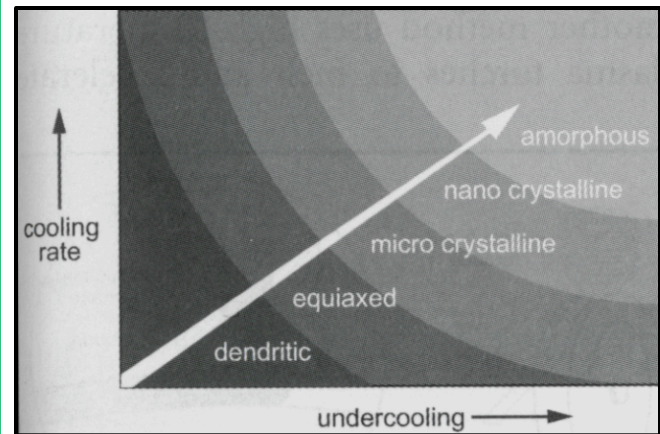
As-Atomized Microstructure (SEM)



Mote Isolation

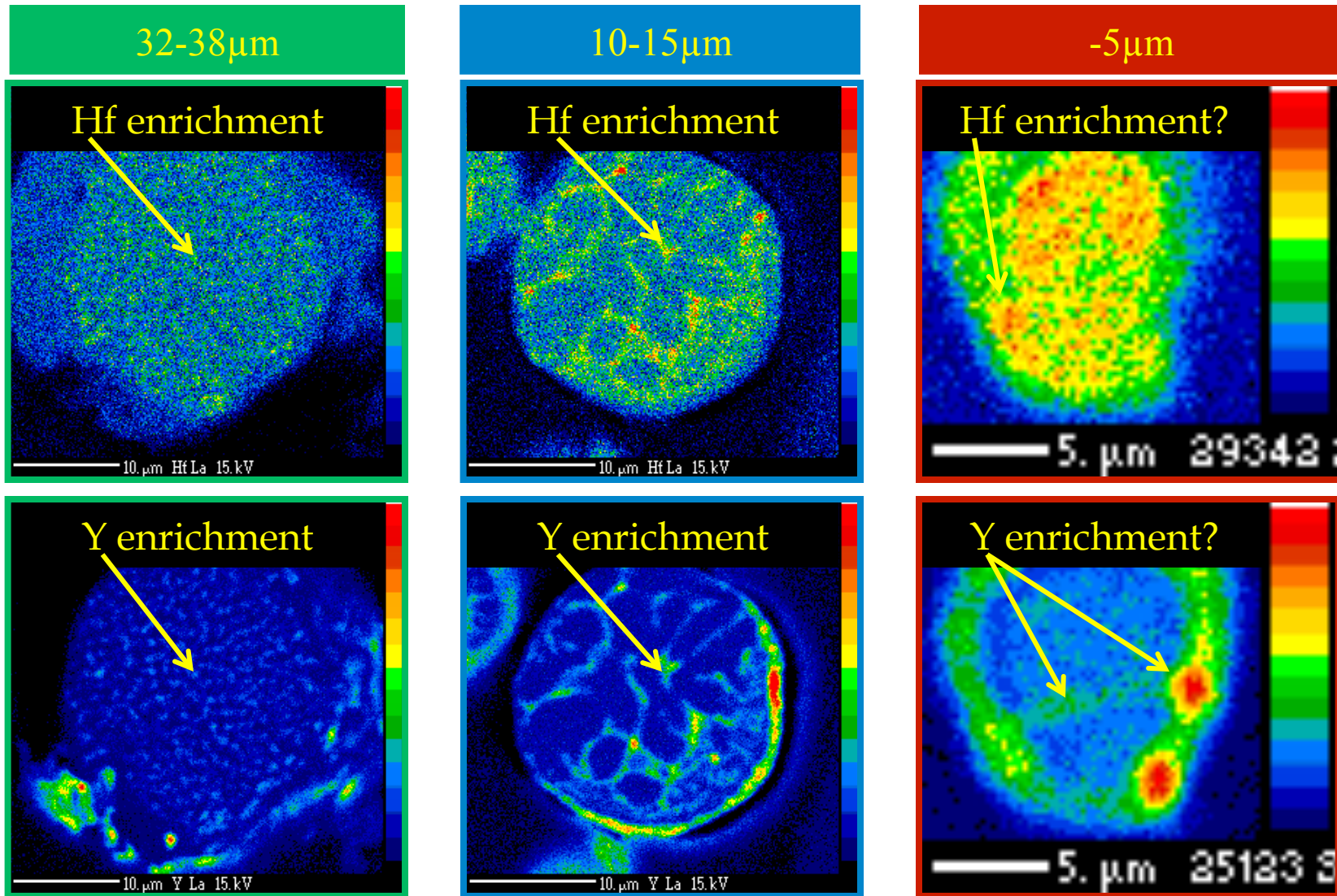


I.E. Anderson, et al., *Undercooled Alloy Phases*, TMS-AIME, 1986, p. 269-285



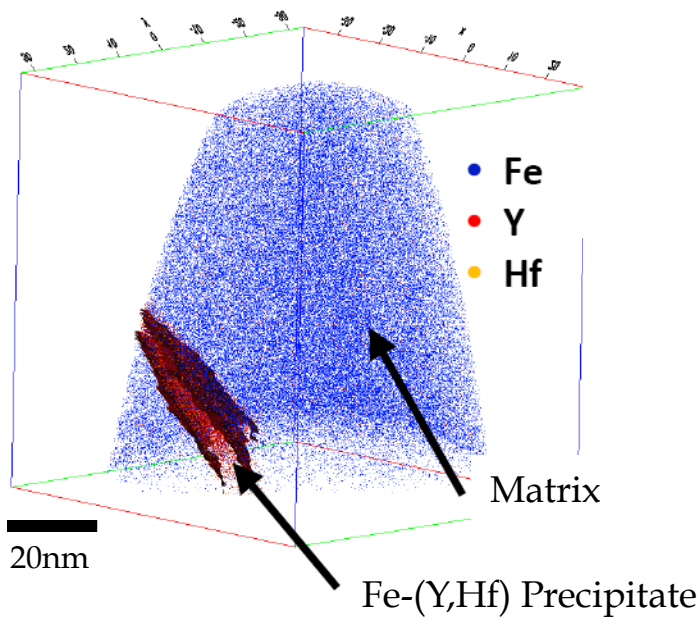
R.M. German, *Powder Metallurgy and Particulate Materials Processing*, 2005, MPIF, Princeton, NJ.

As-Atomized Microstructure (EPMA)*

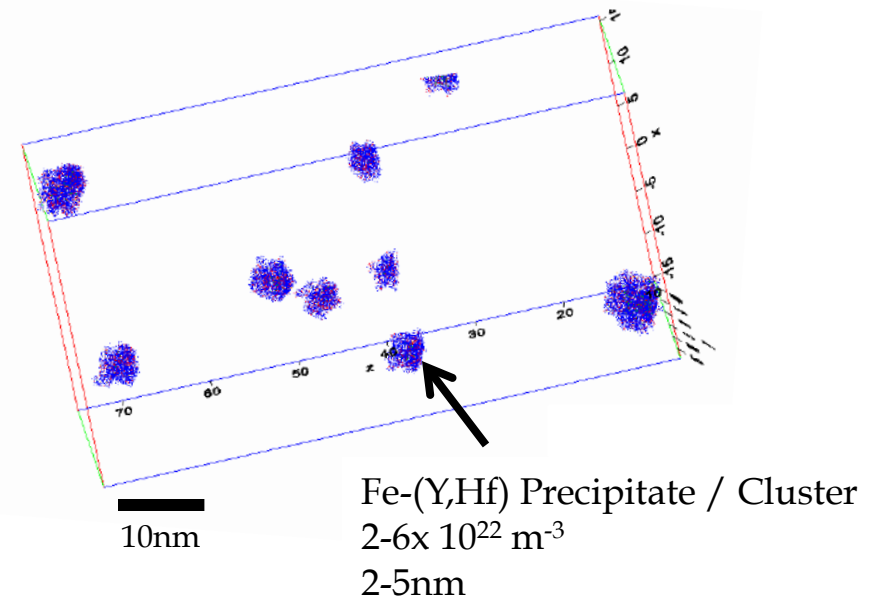


As-Atomized Microstructure: Atom Probe Tomography*

~15 μ m Particle



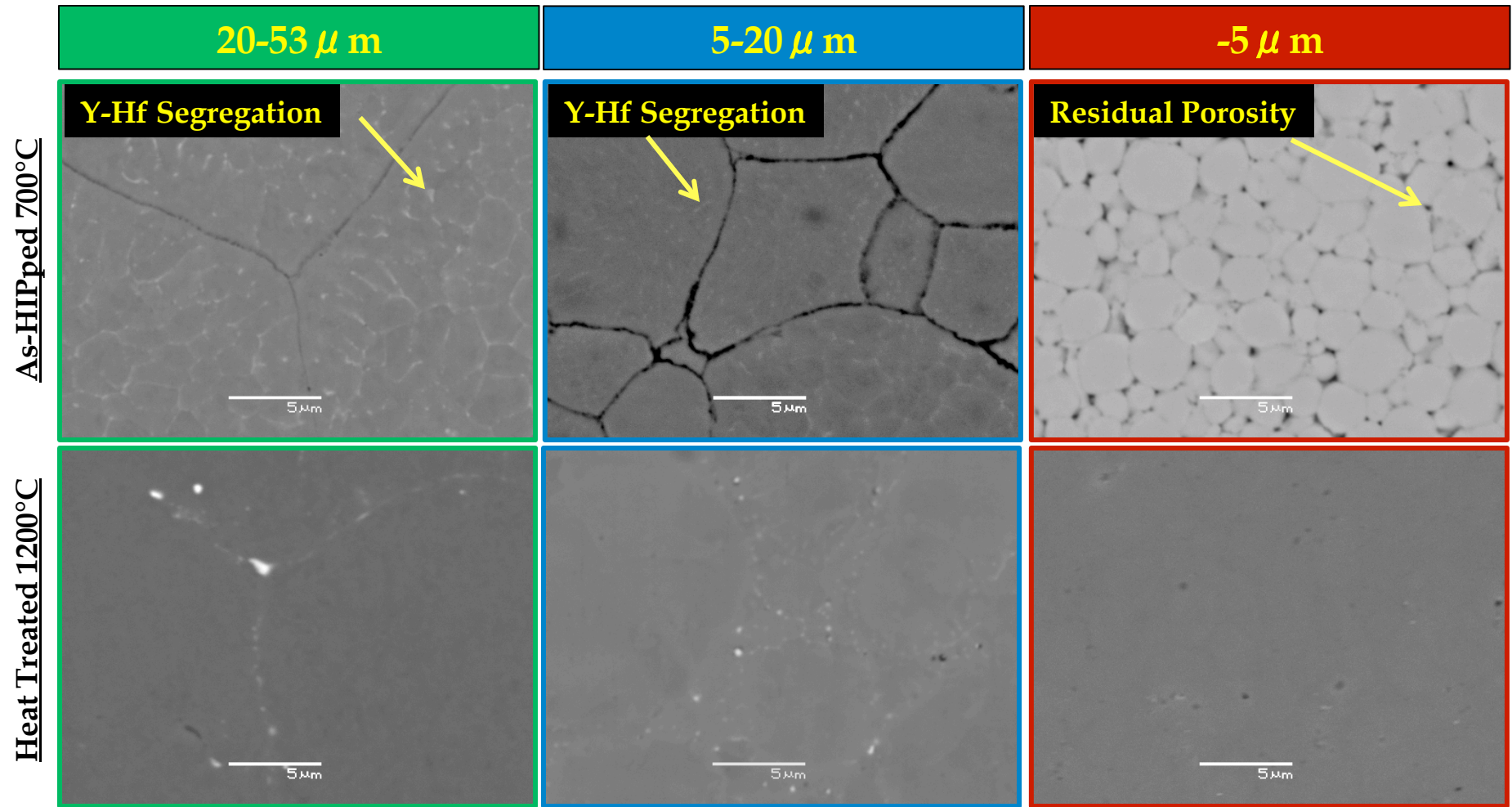
~5 μ m Particle



	Fe	Cr	Y	Hf	O	H		Fe	Cr	Y	Hf	O	H
Nominal	Bal.	15.84	0.18	0.11	0.38	-	Nominal	Bal.	15.84	0.18	0.11	0.38	-
Matrix	Bal.	15.72	0.02	0.01	0.01	0.02	Matrix	Bal.	16.81	0.01	0.01	0.02	0.01
Precipitate	Bal.	11.58	4.86	2.93	0.00	2.00	Precipitate	Bal.	11.78	6.25	5.18	0.01	5.18

Microstructure Evolution (SEM)

CR-156Y-Hf: Fe-15.84Cr-0.11Hf-0.18Y at.%



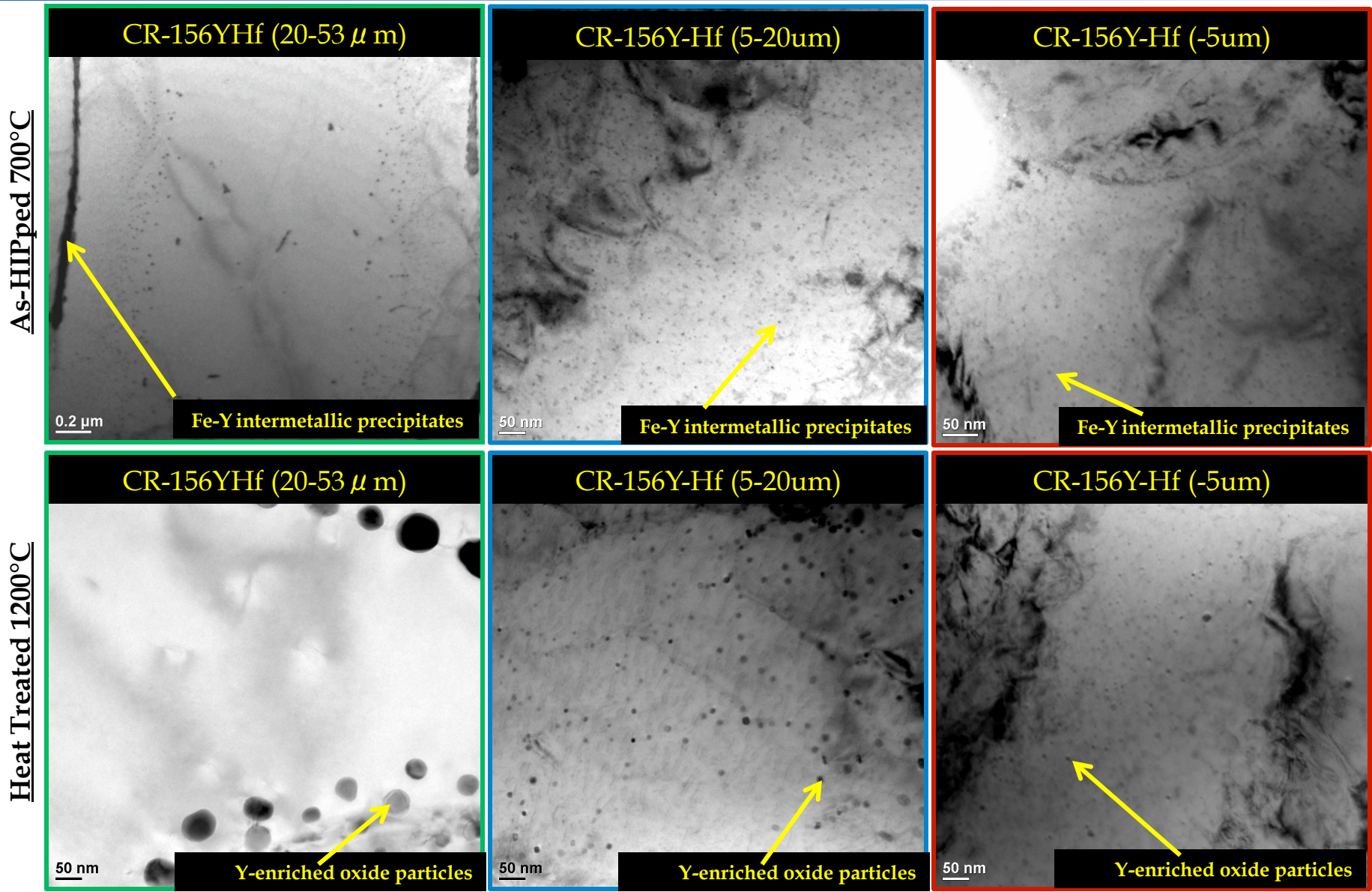
Increasing Total Oxygen Content



Decreasing Residual Intermetallic Precipitates

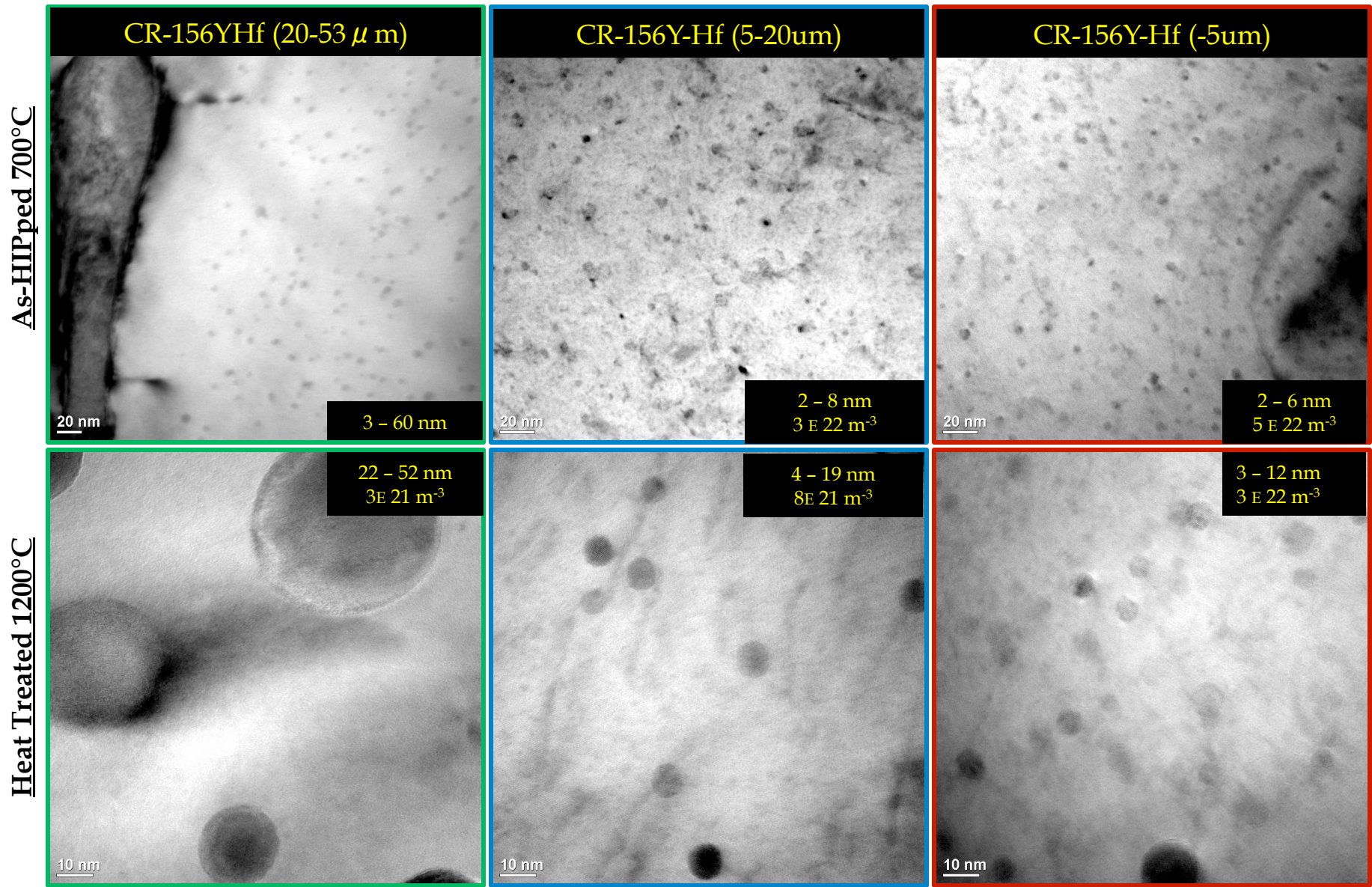
Microstructure Evolution (TEM)

CR-156Y-Hf: Fe-15.84Cr-0.11Hf-0.18Yat.%



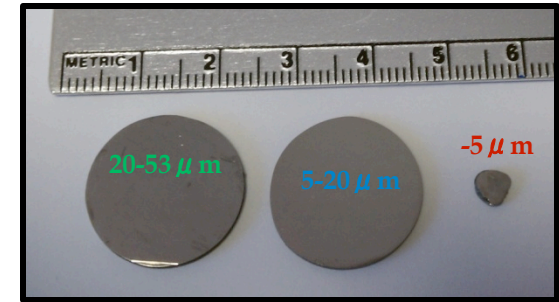
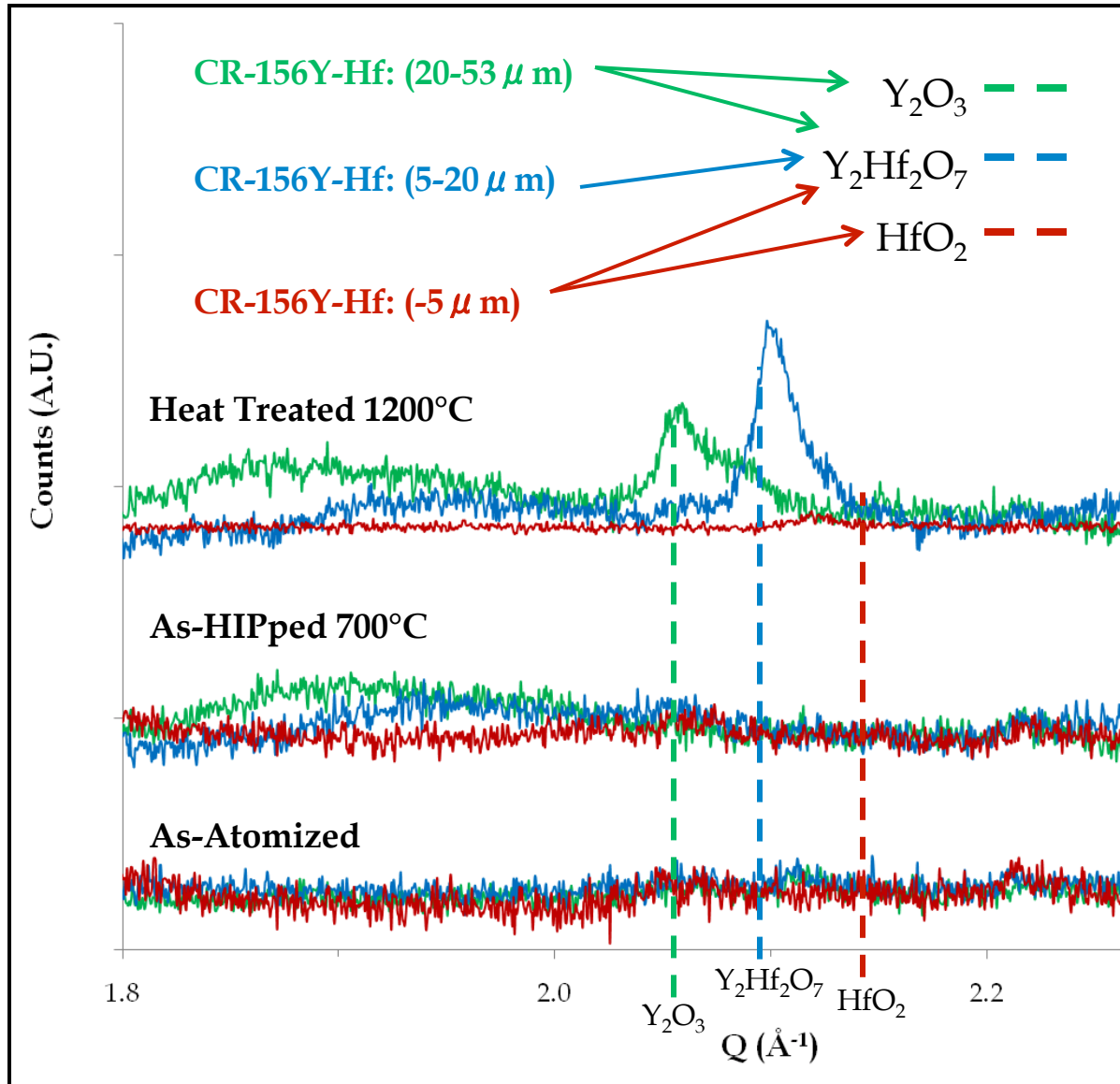
Microstructure Evolution (TEM)

CR-156Y-Hf: Fe-15.84Cr-0.11Hf-0.18Yat.%



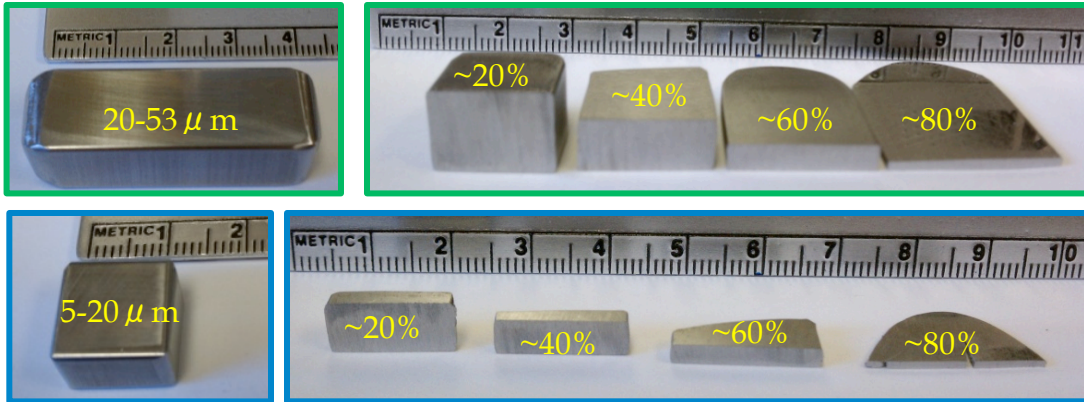
XRD Characterization of Dispersoid Formation

CR-156Y-Hf: Fe-15.84Cr-0.11Hf-0.18Y at.%



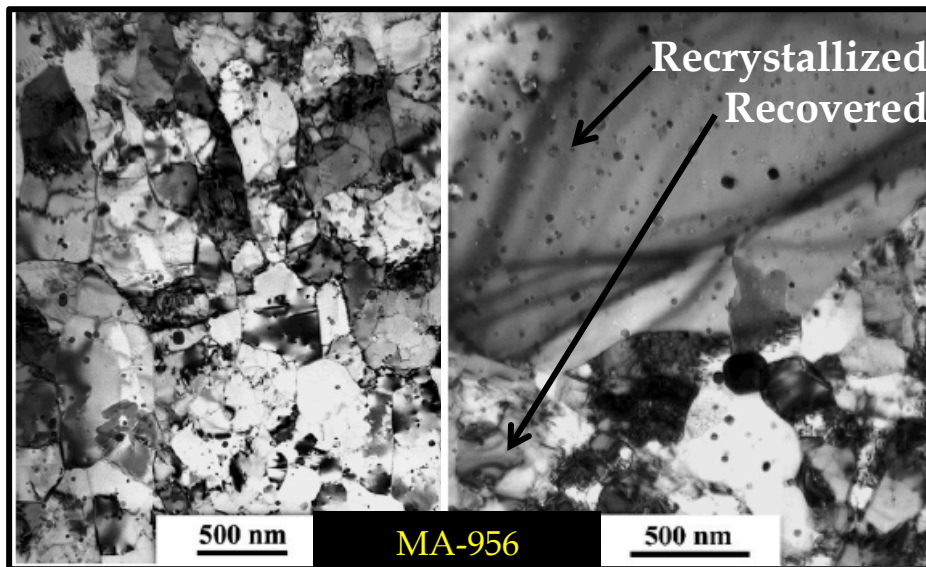
- Dispersoid phase formation seems related to precursor intermetallic composition
- To be confirmed using HE-XRD

Dislocation Substructure Development

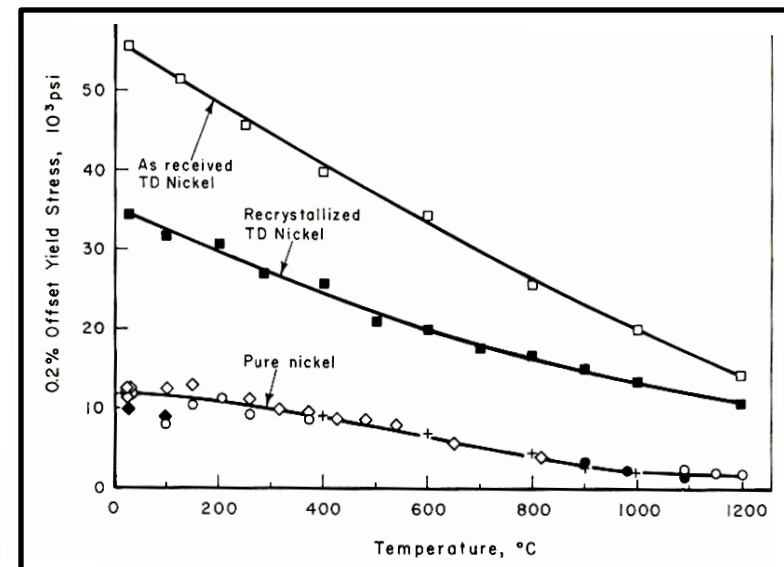


TMT Procedure

- As-heat treated 1200°C - 2.5hr (~0.45 vol.% oxide dispersoid phase)
- Cold Rolled to 80% RA (~10% RA per pass)
- Annealed at 500 or 600°C for 1hr (dislocation recovery)

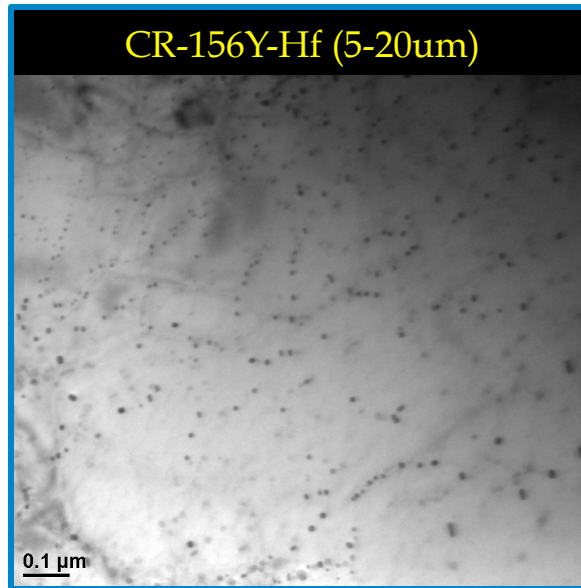
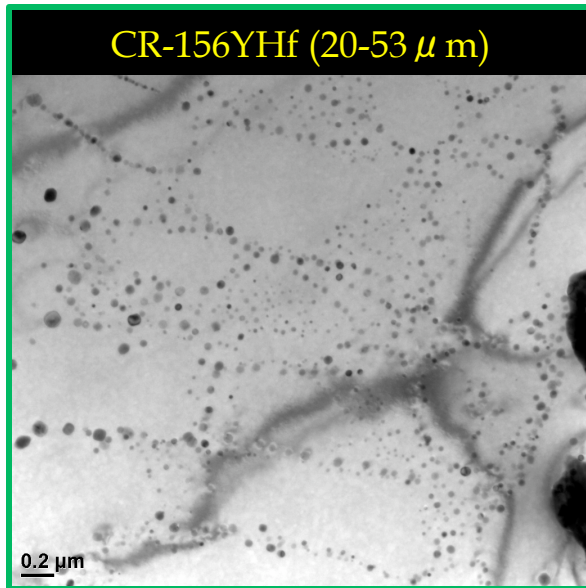


M.F. Hupalo, et al., ISIJ Inter., 2004. 44(11)

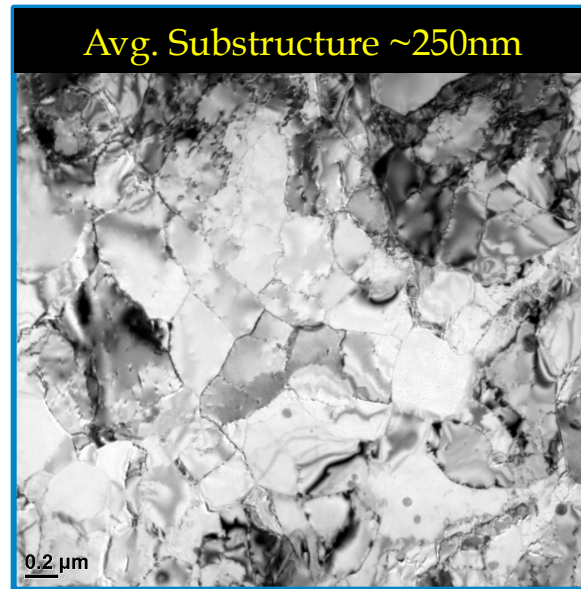
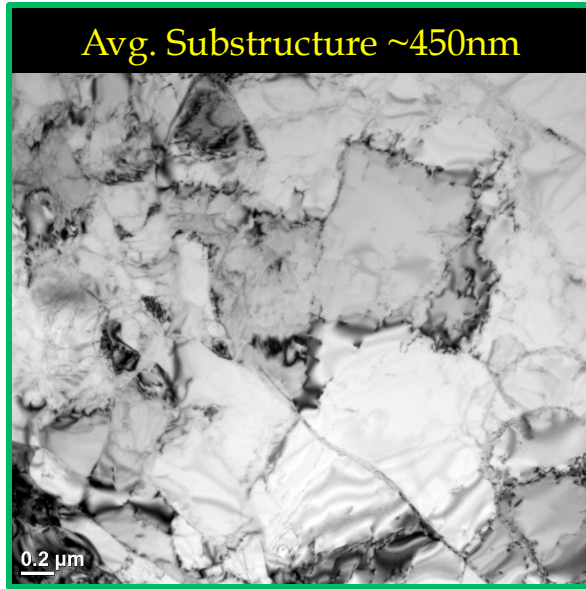


B.A. Wilcox, et al., in *Strength of Metals and Alloys*. 1967.

Dislocation Substructure Development



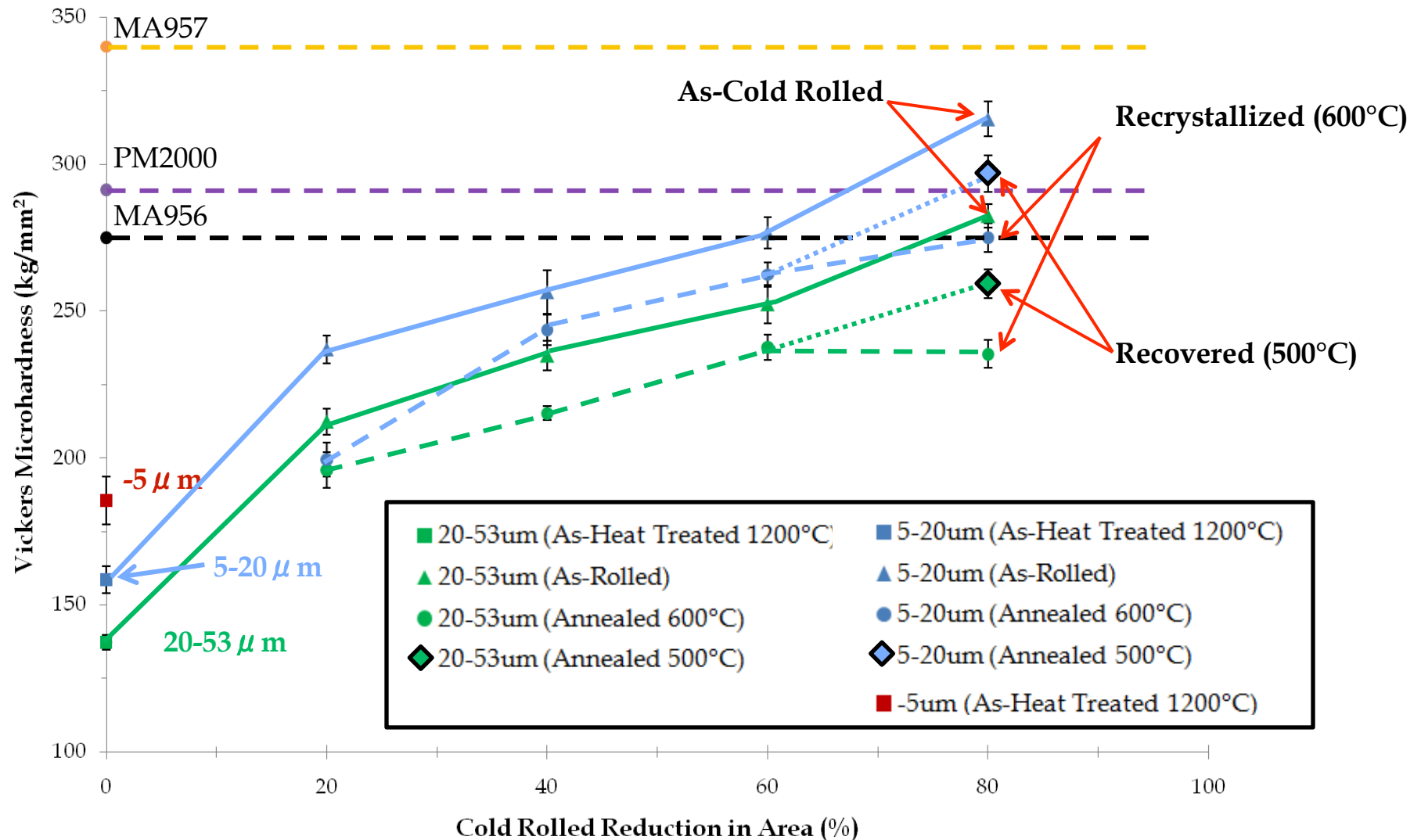
**As-Reacted
ODS Microstructure
(Heat Treated 1200°C)**



**Cold Rolled 80% RA
Annealed 500°C-1hr
(Dislocation Recovery)**

Vickers Microhardness Results

CR-156Y-Hf: Fe-15.84Cr-0.11Hf-0.18Y at.%



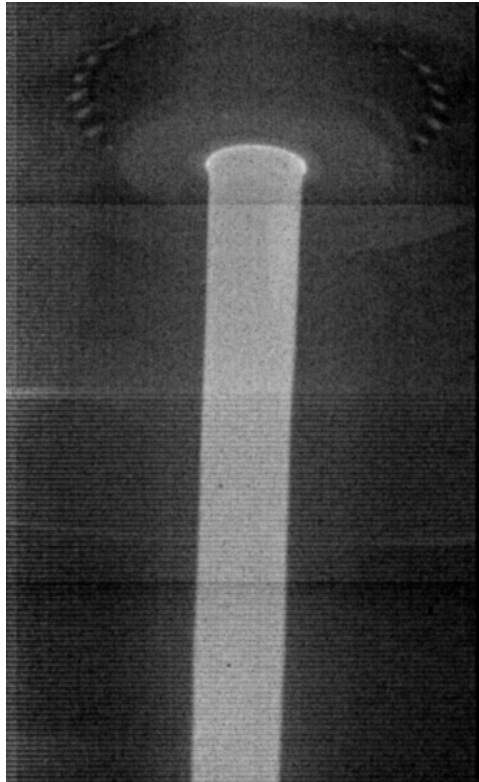
CR-Alloy Microstructure Summary

- A new simplified processing* technique involving gas atomization and in situ oxidation has been developed to produce precursor ferritic stainless steel powder that can be consolidated into an oxide dispersion strengthened alloy with an equiaxed microstructure.
- Resulting oxygen content was successfully predicted using an empirically developed linear processing model, depending inversely on particle size.
- Phase analysis confirmed that nano-metric Y-enriched oxide dispersoids formed by oxygen release/transport/reaction with intermetallic particles or dissolved solute during elevated temperature heat treatment.
- Resulting ODS microstructures were shown to be cellular/dendritic with cell spacing inversely dependent on powder particle size (i.e., rapid solidification rate).
- Particles with maximum amount of solute trapping ($<5 \mu\text{m}$) resulted in smaller and more evenly distributed nano-metric oxide dispersoids.
- Selection of powder particle size range (solidification morphology) was shown to be a viable method to control the final ODS microstructure.
- Thermal-mechanical processing was used to develop a fine scale dislocation substructure, which resulted in significant increases ($\sim 2X$) in alloy microhardness, as a preliminary test of ultimate mechanical properties.

Analysis of Atomization Melt Flow Control by Orifice Design

High Speed Video: Atomization of Fe-Based ODS Alloys

GA-1-162: Straight



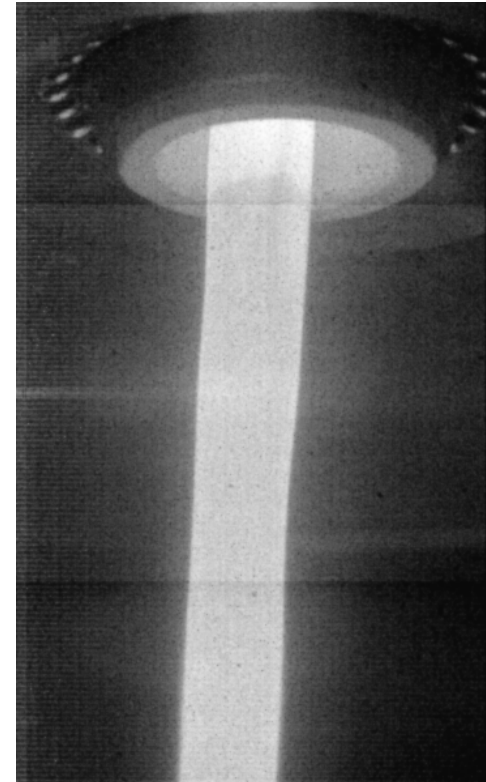
2000fps

GA-1-164: Trumpet + 4 Slots



4000fps

GA-1-166: Trumpet



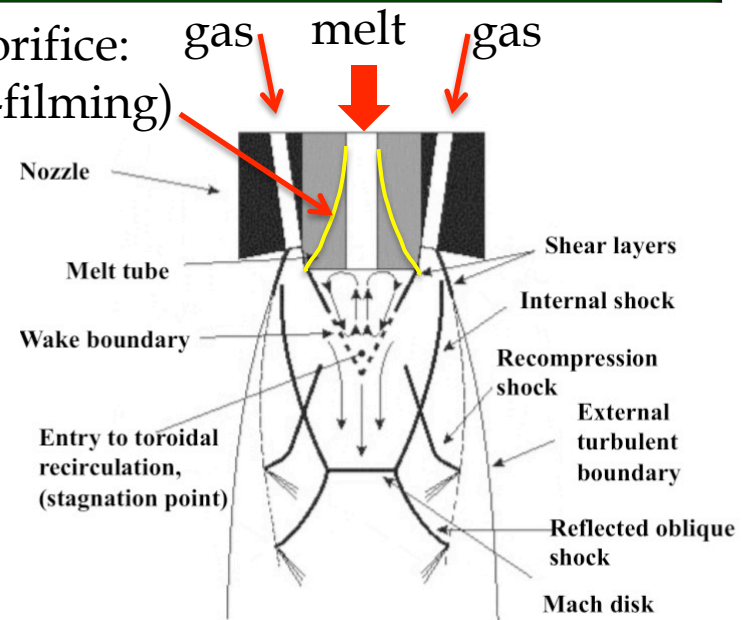
8000fps

Effect on Oxidation Reaction

Alloy		Fe (at. %)	Cr (at. %)	Hf (at. %)	Y (at. %)	O (at. %)	Rxn Gas (vol.%)	Rxn Gas Inlet
CR-164HfY	-20 μ m	Bal.	15.55	<u>0.12</u>	<u>0.09</u>	1.04	Ar-0.19O ₂	HPGA Nozzle
CR-166TiY	-20 μ m	Bal.	15.91	<u>0.12</u>	<u>0.09</u>	<u>0.49</u>	Ar-0.19O ₂	HPGA Nozzle

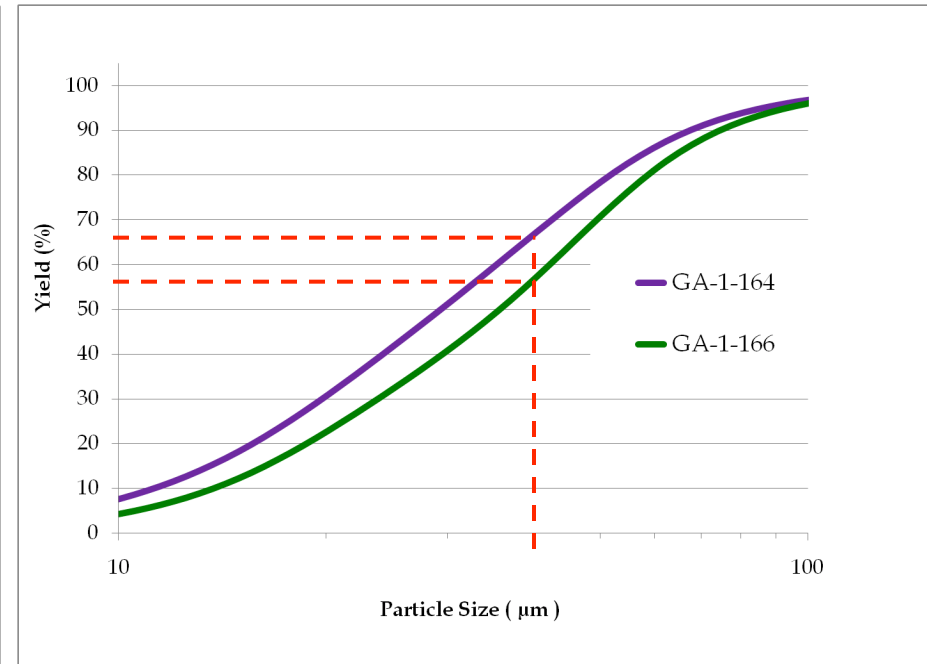
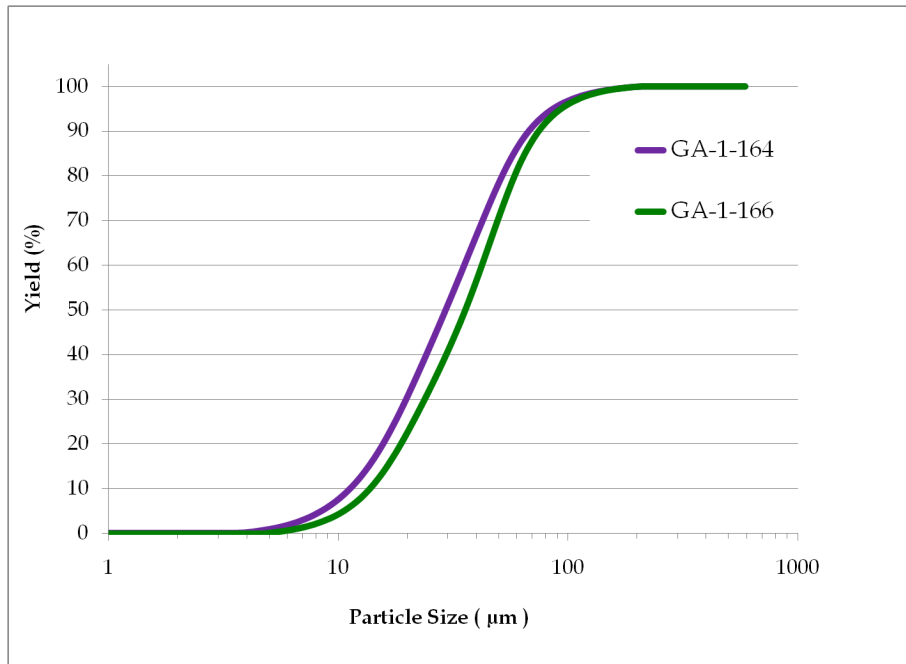
Trumpet bell profile for melt orifice: gas melt gas
 melt follows interior wall (pre-filming)

- **Rapid oxidation kinetics in atomization spray**
- **Primarily dependent on the mass flow rate of oxygen (local p_{O_2} within primary atomization zone)**
- **Sensitive to atomization parameters (gas nozzle and pour tube design)**
- **Longer residence time within pre-filming regime at high p_{O_2} within trumpet bell pour tube increases oxygen content**



J. Ting and I.E. Anderson, Mat. Sci. Eng., A379 (2004), 264-276.

Powder Yield Results

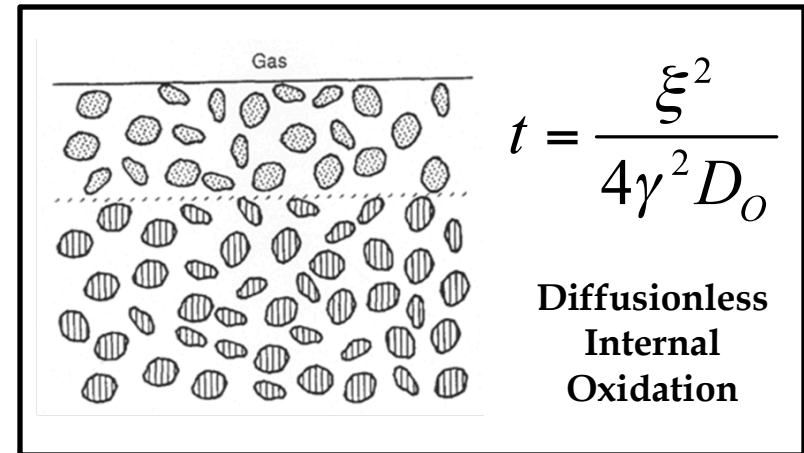


- Cut -106µm
- Riffled (statistical sampling)
- Microtrac analysis

Example:

Alloy	Powder Size (um)	Yield (%)
CR-164HfY	40	67
CR-166TiY	40	57

Recent Consolidation and Dispersoid Formation



- HIPped 700°C - 300MPa - 4hrs (full consolidation, intermetallic precipitation, and restricted oxygen exchange reaction)
- Heat treated at 1200°C - 2.5hrs - Vac. (dispersoid formation through internal oxidation of precursor intermetallic precipitates), predicted using internal oxidation model (Rapp) and experimental results (Rhines packs)
- Samples intended for mechanical testing at elevated temperature (key milestone)

Coarsening Experiment In-Progress

Coarsening schedule for both CR-164HfY and CR-166TiY

Temperature (°C)	Time (hr)
1200	50
1200	100
1200	500
1200	1000*

* Analysis in progress.....

- Determine dispersoid thermal stability (Y-Hf-O vs. Y-Ti-O)
- XRD analysis (Scherrer analysis)
- TEM analysis (line intercept)

$$t \approx \frac{k\lambda}{\beta \cos \theta_{\beta}}$$

(peak broadening)

Acknowledgments

- ❖ *Support from the Department of Energy-Office of Fossil Energy is gratefully acknowledged through Ames Laboratory contract no. DE-AC02-07CH11358.*

• *Jim Anderegg¹, Elliot Fair², and Alex Spicher²*

• *Dr. Robert Odette³, Dr. Erich Stergar³, and Erin Haney³*

• *Jon Hiller⁴ and Dr. Russ Cook⁴*

¹Division of Materials Sciences and Engineering, Ames Laboratory (USDOE)

²Iowa State University, Material Science and Engineering (Undergraduate Students)

³University California Santa Barbara, Mechanical and Environmental Engineering

⁴Electron Microscopy Center for Materials Research, Argonne National Laboratory (USDOE)

